

02

Optical properties of Ga–Ge–Sb–Se chalcogenide glasses doped with terbium and dysprosium ions, near the fundamental absorption band edge

© Yu.S. Kuzyutkina¹, N.D. Parshina¹, E.A. Romanova¹, V.I. Kochubey¹, M.V. Sukhanov²,
L.A. Ketkova², V.S. Shiryaev²

¹ Saratov National Research State University,
410012 Saratov, Russia

² G.G. Devyatikh Institute of Chemistry of High-Purity Substances of RAS,
603951 Nizhny Novgorod, Russia

e-mail: kuzyutkina_y@mail.ru, fiz@sgu.ru, shiryaev@ihps-nnov.ru

Received September 5, 2022

Revised October 7, 2022

Accepted December 30, 2022

In the paper, results of measurements of the optical response of chalcogenide glasses of the $\text{Ga}_5\text{Ge}_{20}\text{Sb}_{10}\text{Se}_{65}$ composition doped with rare-earth ions Tb^{3+} or Dy^{3+} , in the wavelength range of $0.7\text{--}1.5\ \mu\text{m}$ by the method of IR spectroscopy are presented. Parameters characterizing the fundamental absorption band edge of the glasses — optical bandgap energy, Urbach tail parameter and weak absorption tail parameter — have been evaluated. It has been found that doping in low concentrations (up to 0.3 wt%) does not influence the optical bandgap energy and optical properties of the glasses in the range of the Urbach tail, but in the range of the weak absorption tail, optical response of the glasses depends on the activator concentration. Crystallization of the glasses produced by the direct melting method also depends on the activator concentration. In the glasses doped with Dy^{3+} , absorption bands of the ion are located in the range of the weak absorption tail of the glass that makes possible energy transfer between the ions and the gap states of the charge carriers.

Keywords: rare earth elements, chalcogenide glasses, bandgap energy, Urbach tail, weak absorption tail, gap states.

DOI: 10.21883/EOS.2023.01.55511.4083-22

1. Introduction

Chalcogenide glasses (CGs) — are glassy semiconductors [1], which contain one or more chalcogens (Se, S, Te), arsenic (As), germanium (Ge), gallium (Ga), antimony (Sb) and other elements. Chalcogenide glasses are characterized by low optical losses in the wavelength range from 0.5 to $20\ \mu\text{m}$, depending on the composition of the glass. Rare earth elements (REE) are elements of the group III of the Mendeleev's table of chemical elements with atomic numbers 21, 39, 57, 58–71: scandium, yttrium, lanthanum and 14 lanthanides. Terbium (Tb) and dysprosium (Dy) are lanthanides with atomic numbers 65 and 66. Optical fibers from CGs, doped with REE ions are used in the design of infrared (IR) lasers and amplifiers, as well as broadband radiation sources [2,3]. In the bulk samples of CGs, doped with Tb^{3+} , Pr^{3+} and Ce^{3+} [4], and in chalcogenide fibers doped with Tb^{3+} [5,6], lasing was demonstrated in the wavelength range $5\text{--}5.5\ \mu\text{m}$. On the basis of a chalcogenide fiber doped with Pr^{3+} , a luminescent source at wavelengths of $4.0\text{--}5.5\ \mu\text{m}$ was created, which was successfully tested in the fiber-optic sensor system [7].

With extensive studies of the luminescence of REE ions in various CGs matrices in the mid-IR range, the effect of the activator on the optical properties of doped CGs

near the edge of the fundamental absorption band (FAB) has not been sufficiently studied to date. For the CGs, this is the range from 0.8 to $2\ \mu\text{m}$ in the near IR. In the same region lie the absorption bands of REE ions, which are usually used to excite luminescence by available laser sources. It is well known that the characteristic lifetimes of energy levels and transition frequencies of REE ions have different values in CGs of different composition [8]. When studying the shape of the FAB edge of doped glasses with different concentrations of REE ions, it is possible to determine the parameters characterizing the electronic properties of the glasses — the optical band gap energy, the parameter of the Urbach region and the parameter of the weak absorption region. These regions, in which the absorption coefficient decreases exponentially with a decrease in the photon energy, arise due to the absorption of radiation with the participation of bound states inside the band gap of CGs. The bound states of charge carriers correspond to structural features in the molecular lattice of CGs: these are homopolar and broken bonds, as well as unshared pairs of p electrons on the outer shell of chalcogen atoms [1,9].

If the transition frequencies inside the band gap and the transition frequencies in REE ions coincide, then at the moment when radiation is absorbed at the Urbach tail or at

Table 1. REE content in glasses according to the ICP-AES results

| REE | Measured REE content, wt% | Deviation from weighted quantities, % | Nominal mass concentration-concentration C , wt% |
|-----|---------------------------|---------------------------------------|--|
| Tb | < 0.00001 | 0 | 0 |
| | 0.112 ± 0.002 | 13 | 0.1 |
| | 0.226 ± 0.005 | 12 | 0.2 |
| | 0.331 ± 0.007 | 11 | 0.3 |
| Dy | < 0.0001 | 0 | 0 |
| | 0.108 ± 0.002 | 11 | 0.1 |
| | 0.211 ± 0.004 | 2 | 0.2 |
| | 0.310 ± 0.007 | 2 | 0.3 |

the weak absorption tail, the non-radiative energy transfer between REE ions and bound states in the band gap of CGs [10,11] is possible. The study of the parameters characterizing the FAB edge of doped CGs will make it possible to find out whether energy exchange between bound states and REE ions is possible, and also to establish whether zone-zone transitions and transitions inside the band gap of glass depend on the ion concentration. Such studies are important for optimizing pumping and increasing the quantum yield of luminescence.

In this paper, studies of the shape of the FAB edge for the CGs composition $\text{Ga}_5\text{Ge}_{20}\text{Sb}_{10}\text{Se}_{65}$, doped with ions Tb^{3+} and Dy^{3+} (ion content from 0 to 0.3 wt%) are presented. The glasses were obtained by direct melting of especially pure substances: Ga, Ge, Sb — 6N, Se — 5N, Tb and Dy — 3N [12,13]. The loading of the glass components was carried out in the air and without additional cleaning. The charge was melted in evacuated quartz ampoules at a pressure of 10^{-3} Pa and a temperature of 850°C for 5 h in a rocking furnace. The hardening was carried out in the air. To relieve mechanical stresses, the samples were annealed at a temperature of $T_g + 30^\circ\text{C}$ (T_g — glass transition temperature) for 30 min. Thus, two series of the glasses composition $\text{Ga}_5\text{Ge}_{20}\text{Sb}_{10}\text{Se}_{65}$ were obtained, doped nominally 0, 0.1, 0.2, 0.3 wt% by Tb and Dy, in the form of cylindrical rods weighing 15–40 g, diameter 9–12 mm and length 50–80 mm.

The REE content in the obtained glasses was determined by the Inductively Coupled Plasma - Atomic Emission Spectroscopy (ICP-AES) [14]. The analysis was performed on an iCAP 6300Duo polychromator spectrometer (ThermoScientific, USA). For this purpose, glass samples weighing 100–150 mg from the central part of cylindrical rods were used. The content of terbium and dysprosium in synthesized glasses, determined by the ICP-AES method, differs slightly from the set value (Table 1). This is

due to a large error (4–30 mg) weighing of small REE concentrations.

The glass samples with which the transmission spectra were measured in the mid-IR range on the Tensor 27 IR Fourier spectrometer were cut into rods with a length ~ 20 mm. For measurements near the FAB edge with absorption of more than 10 cm^{-1} , disks with a thickness of 1 mm with plane-parallel sides were made of glass rods polished on both sides. The spectra were measured using a Perkin Elmer Lambda 950 spectrometer in the wavelength range of $0.5\text{--}1.5\ \mu\text{m}$ in the mode of measurement of directional transmission and directional reflection (without an integrating sphere). The micro-heterogeneity of the glasses (the presence of crystals and heterophase inclusions of micron size) was determined by optical microscopy. Measurements were carried out on an Axio Imager microscope M2m with a monochrome camera, sensitive in the visible and near IR ranges, in transmission and reflection modes.

To determine the parameters of the FAB edge of the studied glasses, the technique described in [15] was used. For each sample with a given concentration of the REE ion, the spectral dependences of the absorption coefficient and refractive index in the wavelength range $\lambda = 0.5\text{--}1.5\ \mu\text{m}$ were calculated and determined: the optical band gap energy (E_g), the parameter of the Urbach tail (E_U) and the parameter of the weak absorption tail (E_W).

2. Measurement results

Fig. 1, *a, b* shows the transmission spectra of $T(\lambda)$ measured for undoped samples of the composition $\text{Ga}_5\text{Ge}_{20}\text{Sb}_{10}\text{Se}_{65}$, and for samples of the same composition doped with Tb^{3+} and Dy^{3+} with $C = 0.3$ wt%. It can be seen that the absorption bands of the doped samples correspond to the wavelengths of transitions between the energy levels of terbium or dysprosium (Fig. 1, *c, d*). The intensities of the absorption bands of these transitions are different according to the different absorption cross-sections of the REE ion [16]. The observed absorption band in the region $\lambda = 4.5\text{--}4.6\ \mu\text{m}$ in the spectra of both doped and undoped glasses arises due to the presence of a Se–H bond due to the presence of impurity hydrogen [17].

Optical pumping of glasses doped with Tb^{3+} , is usually performed in the absorption band with $\lambda = 2\ \mu\text{m}$, and infrared luminescence occurs from the levels 7F_4 and 7F_5 at wavelengths 3 and $5.1\ \mu\text{m}$. For glasses doped with Dy^{3+} , pumping is usually performed in the near IR range in absorption bands with $\lambda \approx 0.8$ [18], 0.9, 1.1 and $1.3\ \mu\text{m}$ [19], and luminescence is observed at wavelengths 3.2 and $4.6\ \mu\text{m}$. In the CGs doped with Tb^{3+} and Dy^{3+} , there are other radiative transitions at other wavelengths in the mid IR [8], which are not shown in Fig. 1, *c, d*.

Transmission spectra measured near the FAB edge transmission $T(\lambda)$ and reflection $R(\lambda)$ of the samples of glasses

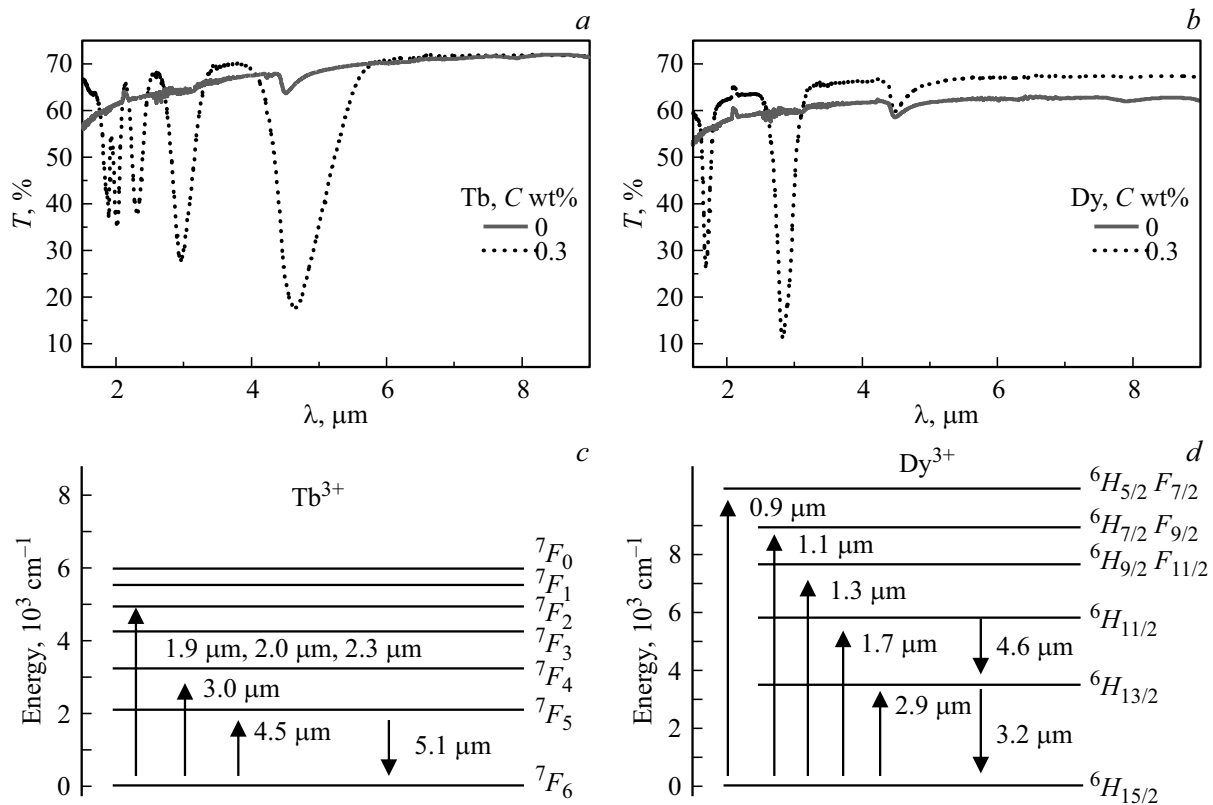


Figure 1. Measured transmission spectra of samples of undoped glasses of the composition $\text{Ga}_5\text{Ge}_{20}\text{Sb}_{10}\text{Se}_{65}$ and samples of the same composition doped with Tb^{3+} (a) and Dy^{3+} (b). Energy levels and wavelengths of transitions of Tb^{3+} (c) and Dy^{3+} (d).

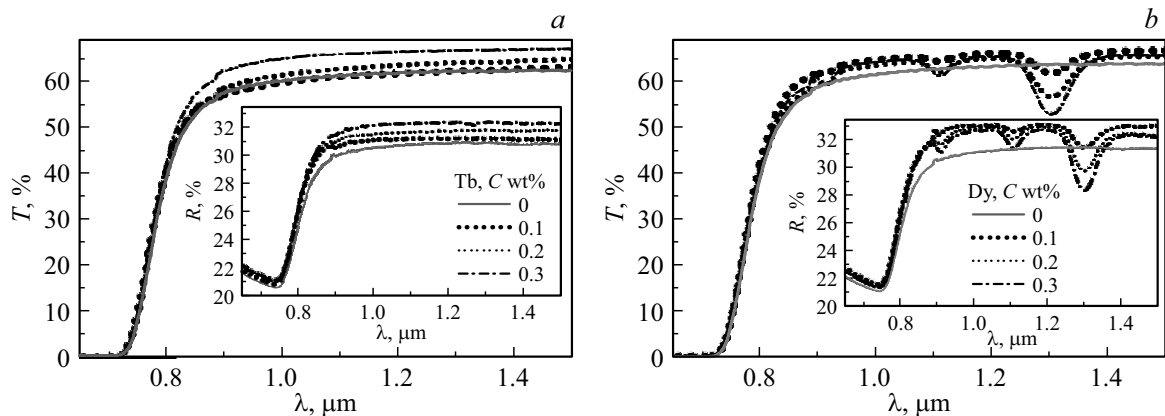


Figure 2. Measured transmission and reflection spectra (inset) of samples of undoped glasses of the composition $\text{Ga}_5\text{Ge}_{20}\text{Sb}_{10}\text{Se}_{65}$, and samples of the same composition doped with Tb^{3+} (a) and Dy^{3+} (b).

of the composition $\text{Ga}_5\text{Ge}_{20}\text{Sb}_{10}\text{Se}_{65}$, and also samples of the same composition doped with Tb^{3+} and Dy^{3+} with $C = 0.1, 0.2$ and 0.3 wt%, are shown in Fig. 2. Noises in the wavelength range $0.8\text{--}0.9 \mu\text{m}$ are associated with the operation mode of the spectrophotometer (switching of gratings in the spectrophotometer, as well as changing the source and detector of radiation). In the $T(\lambda)$ spectra of samples doped with Tb^{3+} , there are no absorption bands in the spectral region under consideration. In the $T(\lambda)$ spectra of samples with Dy^{3+} characteristic

absorption bands with minima at wavelengths $0.9, 1.1$ and $1.3 \mu\text{m}$, corresponding to the absorption transitions of the ion are shown, respectively: ${}^6H_{15/2} \rightarrow {}^6H_{5/2} + {}^6F_{7/2}$, ${}^6H_{15/2} \rightarrow {}^6H_{7/2} + {}^6F_{9/2}$, ${}^6H_{15/2} \rightarrow {}^6H_{9/2} + {}^6F_{11/2}$ [20].

It can be seen from the graphs in Fig. 2 that at a given wavelength in samples with Tb^{3+} , transmission and reflection increase with the growth of concentration C . In the samples with Dy^{3+} , the transmission is expected to decrease in the absorption bands with an increase of C . The transmission between the absorption bands of the undoped

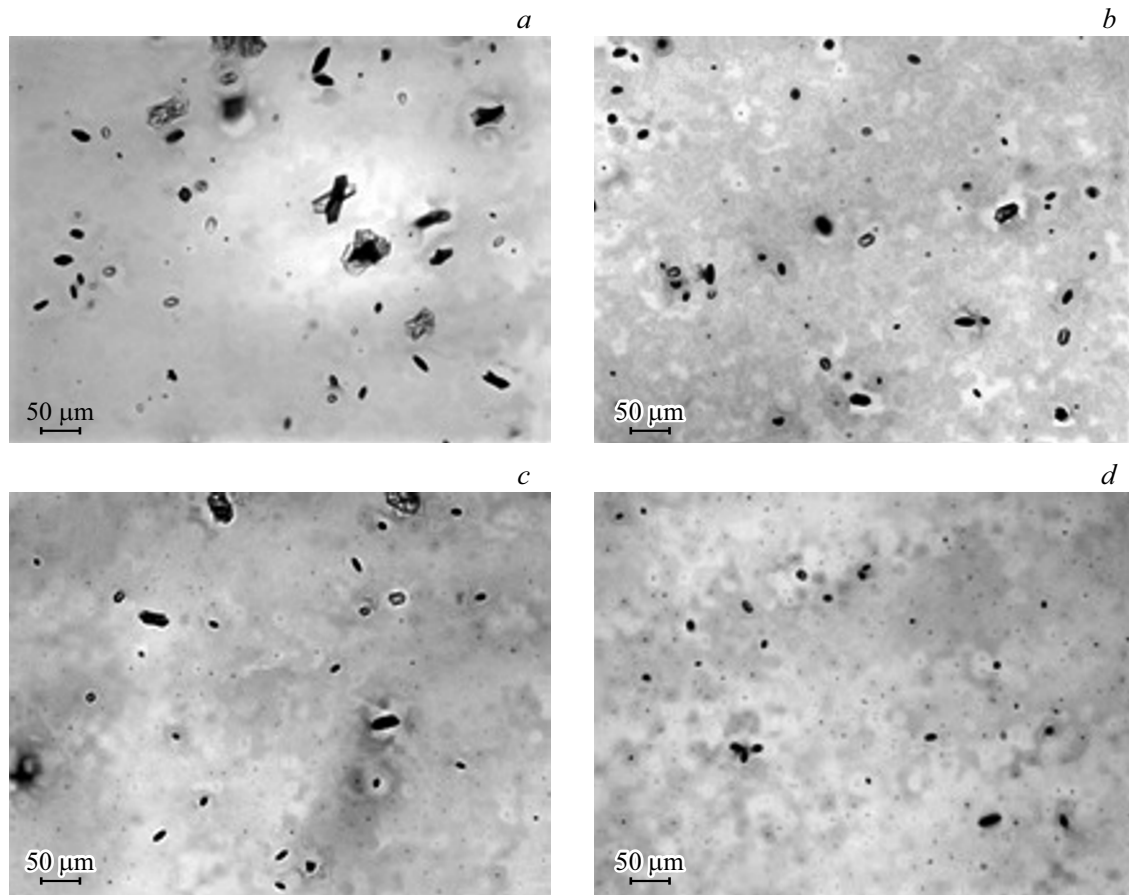


Figure 3. Images of samples obtained in the near IR range for undoped glasses of the composition $\text{Ga}_5\text{Ge}_{20}\text{Sb}_{10}\text{Se}_{65}$ (*a, b*) and doped Tb^{3+} (*c*) and Dy^{3+} (*d*), $C = 0.3 \text{ wt}\%$.

samples is less than that of the doped ones, as in the spectra shown in Fig. 1.

To explain the revealed features in the measured spectra of samples with different concentrations of REE ions, studies of the microstructure of glasses were carried out. Fig. 3 shows microscopic images of samples obtained in the near IR range. The figure clearly shows, as established in [13], GeSe_2 crystals, and the content of such inclusions in undoped samples is noticeably greater than in the doped ones. In the undoped samples from the series with terbium, the diameter of the observed crystals is $3\text{--}55 \mu\text{m}$, and from the series with dysprosium — $2\text{--}36 \mu\text{m}$ (fig. 3, *a, b*). Accordingly, the number of inclusions is equal to $8 \cdot 10^4$ and $9 \cdot 10^4 \text{ cm}^{-3}$. The scattering losses in the wavelength range $1\text{--}7 \mu\text{m}$, determined by the method described in [21], were 160 and 40 dB/m. In the sample doped with Tb^{3+} ions with $C = 0.3 \text{ wt}\%$, the diameter of crystal inclusions is also in the range of $3\text{--}55 \mu\text{m}$, but the number of inclusions is $3 \cdot 10^4 \text{ cm}^{-3}$ is significantly lower than in the undoped sample. The scattering losses are 40 dB/m. In the sample with Dy^{3+} at $C = 0.3 \text{ wt}\%$, the diameter of inclusions in the range $3\text{--}16 \mu\text{m}$, is less than in the undoped one, as is the number of inclusions $4 \cdot 10^4 \text{ cm}^{-3}$. The scattering losses are 15 dB/m.

Thus, according to Fig. 3, as a result of doping glasses of the composition $\text{Ga}_5\text{Ge}_{20}\text{Sb}_{10}\text{Se}_{65}$ with REE ions at a concentration of $C = 0.3 \text{ wt}\%$ the number of crystalline inclusions has decreased compared to undoped glass. Since measurements on a spectrophotometer in the near-IR range were carried out without an integrating sphere, the values of T and R of samples with different concentrations of REE ions are determined not only by the reflection and absorption of radiation in glass samples, but also by the scattering of radiation on crystalline inclusions. The scattering contribution is smaller in samples with fewer crystal inclusions, i.e. with a higher concentration of REE ions. For the same reason, in glasses with Dy^{3+} between the ion absorption bands, the scattering is less in doped samples.

3. Definition of the FAB edge parameters

3.1. Method of processing measurement results

According to the methodology described in [15], a two-dimensional model of a plane light wave incident on a plane-parallel glass plate was used to calculate T and R taking into account multiple reflections from the sample surface with a

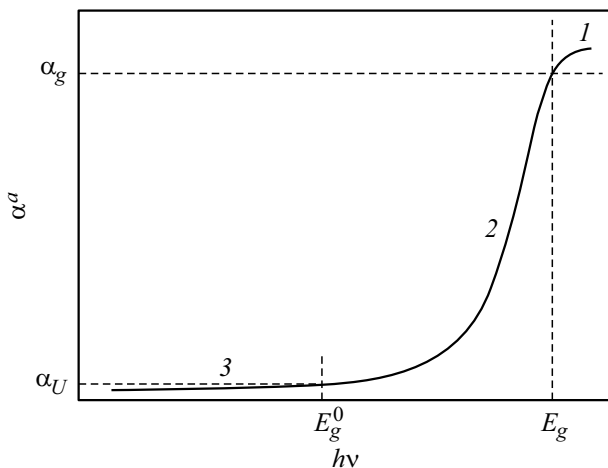


Figure 4. The FAB edge of CGs: 1 — Tautz region; 2 — Urbach tail; 3 — weak absorption tail.

thickness of d . As a result of solving the system of equations for T and R , an expression for the attenuation coefficient can be obtained:

$$\alpha = -\frac{1}{d} \ln \left(\frac{T^2 - (1-R)^2 + \sqrt{4T^2 + ((1-R)^2 - T^2)^2}}{2T} \right), \quad (1)$$

where $\alpha = \alpha^a + \alpha^s$, α^a — absorption coefficient, α^s — scattering coefficient.

Since in the spectrophotometer, when measuring reflection, unpolarized radiation falls on the sample at a small angle $\varphi = 8^\circ$, the Fresnel formula for the s -polarization wave was used to calculate the refractive index n (at small angles, the reflection coefficient practically does not depend on the polarization of the radiation), and expression is obtained

$$n = \sqrt{\cos^2 \varphi \left(\frac{1 + \sqrt{R_{12}}}{1 - \sqrt{R_{12}}} \right)^2 + \sin^2 \varphi}. \quad (2)$$

Here R_{12} — the coefficient of reflection from one face of the plate is defined as

$$R_{12} = \frac{0.5}{2-R} \left(T^2 + 1 + 2R - R^2 - \sqrt{4(R-2)R + (1+2R-R^2+T^2)^2} \right). \quad (3)$$

The obtained expressions allow us to calculate the spectral dependences of the absorption coefficient and the refractive index from the values of T and R , obtained in the measured spectra.

The optical properties of the CGs near the FAB edge are determined by the structural features of the energy zones. As in all non-crystalline semiconductors, there are bound states of charge carriers inside the CGs band gap due to the absence of long-range order in the molecular lattice and the presence of defects (homopolar bonds, broken bonds)

and impurities. Therefore, the dependence of the CGs absorption coefficient on the photon energy $h\nu$ (h — Planck constant, ν — radiation frequency) near the FAB edge (Fig. 4) has an exponential decay region — the Urbach tail. The specificity of CGs is the weak absorption tail [1,9].

In the region $h\nu > E_g$ (Tautz region), the absorption spectrum is described by a parabolic dependence:

$$\alpha^a = \frac{B(h\nu - E_g)^2}{h\nu}, \quad (4)$$

where B — is the proportionality coefficient.

In the region $E_g^0 < h\nu < E_g$ (Urbach tail), the absorption spectrum is described by an exponential function:

$$\alpha^a = \alpha_g \exp \left(\frac{h\nu - E_g}{E_U} \right), \quad (5)$$

where E_U — parameter of the Urbach tail, E_g^0 — photon energy at the boundary of the Urbach tail and the weak absorption tail, $\alpha_g = \alpha^a(h\nu = E_g)$, and E_g actually corresponds to the high-frequency edge of the Urbach tail.

Unlike other non-crystalline semiconductors, CGs at $h\nu < E_g^0$ have a third region — a weak absorption tail. The absorption spectrum here can also be approximately described by an exponential function:

$$\alpha = \alpha_U \exp \left(\frac{h\nu - E_g^0}{E_W} \right), \quad (6)$$

where E_W — parameter of the weak absorption tail, $\alpha_U = \alpha^a(h\nu = E_g^0)$. Usually $\alpha_U \approx 1 \text{ cm}^{-1}$.

The CGs band gap energy can be determined by plotting the dependence $\ln(\alpha^a) = f(h\nu)$ [15]. The linear sections on this graph correspond to the Urbach tail and the weak absorption tail, and the slope of these lines can be used to find the parameters E_U and E_W . By the high-frequency edge $\alpha^a = \alpha_g$ of the linear section of the Urbach tail, the value of E_g can be determined. Since in FAB $\alpha_g \approx .10^3 - 10^4 \text{ cm}^{-1}$, the exact value of E_g is usually obtained from measurements of the optical characteristics of submicron films. For samples of greater thickness, the measured values α^a are much smaller. So, for the CGs samples with a thickness of 1–2 mm, it is not possible to obtain the values of $\alpha^a > 10^2 \text{ cm}^{-1}$ [15]. The Tautz method [22], which is often used to determine the band gap energy, gives accurate values of E_g only for single-crystal semiconductors with a sharp FAB edge. For the CGs, this method does not allow to obtain a sufficiently accurate result, and therefore the value of E_g is determined at a given absorption level. First, an approximate value of E_g' is found for some measured value of α_g' , and is then recalculated for a given value α_g by the formula

$$E_g = E_g' + E_U \ln(\alpha_g / \alpha_g'). \quad (7)$$

The parameters E_U and E_W are determined by the slope of the linear sections of the dependence $\ln(\alpha^a) = f(h\nu)$, respectively, at the Urbach tail and at the weak absorption tail.

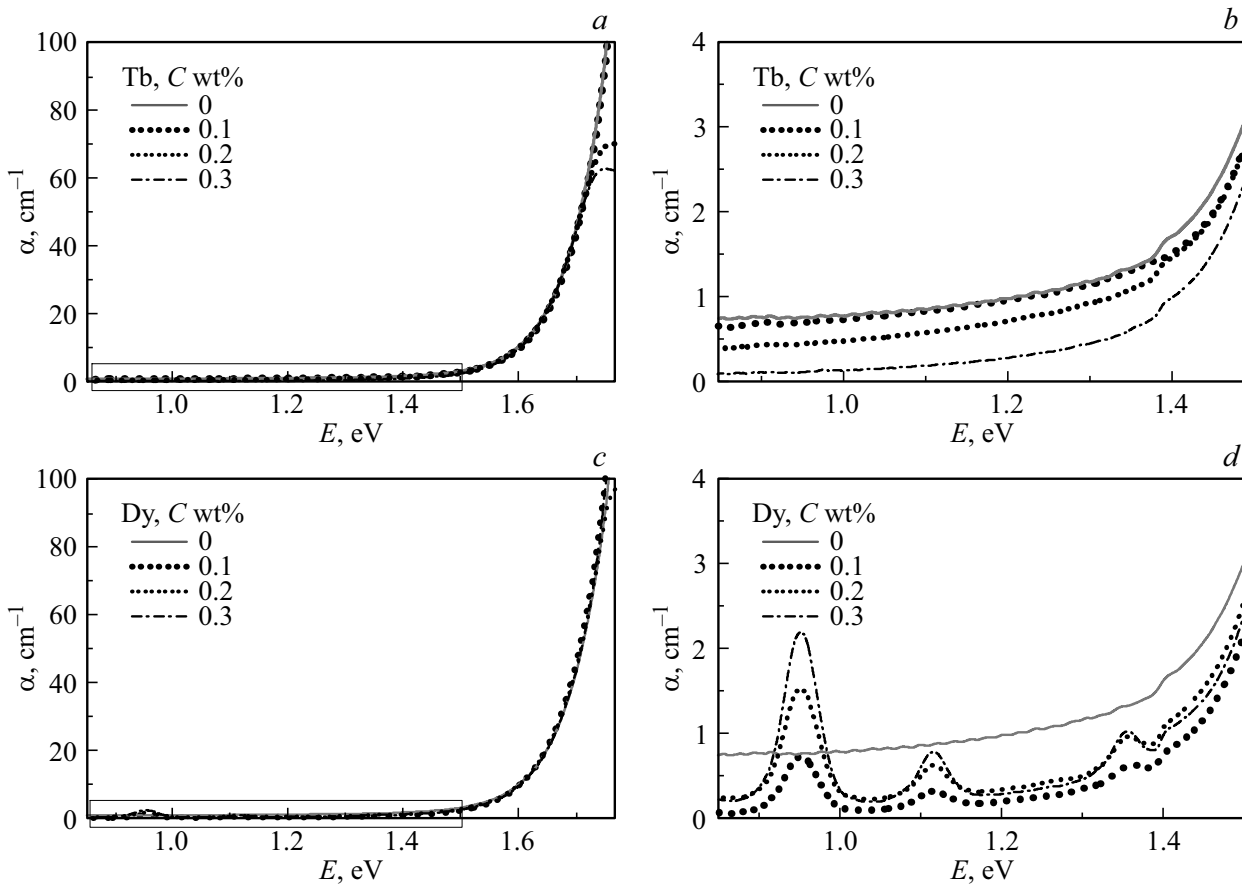


Figure 5. Attenuation coefficient depending on the photon energy calculated for samples of undoped glasses of the composition $\text{Ga}_5\text{Ge}_{20}\text{Sb}_{10}\text{Se}_{65}$ (solid lines) and doped with Tb^{3+} (a) and Dy^{3+} (c). The figures (b) and (d) show the areas highlighted by rectangles in figures (a) and (c).

3.2. Optical properties of glasses near the FAB edge

Fig. 5 shows the dependences of the attenuation coefficient on the photon energy E , calculated by formula (1) for all test samples. Due to the limited sensitivity of the photodetector, it was not possible to obtain values $\alpha > 100 \text{ cm}^{-1}$ when measuring the spectra. We note that in the spectral region under consideration, the value of α^a in samples with Tb^{3+} is determined only by absorption of glass (Fig. 5, a, b), and in samples with Dy^{3+} — by absorption of both glass and dysprosium ions (Fig. 5, c, d).

In Fig. 5, a, d it can be seen that both at the Urbach tail ($E > 1.4 \text{ eV}$) and at the weak absorption tail ($E < 1.4 \text{ eV}$) at a given photon energy, the attenuation coefficient is greater for the undoped glasses than doped glasses (for glasses with Dy^{3+} , regions outside the ion absorption bands are meant), and in samples with Tb^{3+} for a given photon energy, the attenuation coefficient decreases with the growth of C . In the samples, doped with Dy^{3+} , the joint absorption of glass and ion at the weak absorption tail leads to a more complex dependence of $\alpha(C)$ outside the absorption bands.

In ion absorption bands α is expected to grow with its concentration.

The estimates of scattering losses given above in the description to Fig. 3 allow us to determine the value α^s and, thus, to establish the contribution of absorption to the values of the attenuation coefficient in Fig. 5. So, for undoped samples from the series with Tb^{3+} $\alpha^s = 0.37 \text{ cm}^{-1}$, and for undoped samples from the series with Dy^{3+} $\alpha^s = 0.1 \text{ cm}^{-1}$. In the sample doped with Tb^{3+} ions with $C = 0.3 \text{ wt\%}$, $\alpha^s = 0.1 \text{ cm}^{-1}$, and in a sample with Dy^{3+} of the same concentration $\alpha^s = 0.03 \text{ cm}^{-1}$. Then at the wavelength $1 \mu\text{m}$ for samples from the series with Tb^{3+} we get $\alpha^a = 0.41 \text{ cm}^{-1}$ (undoped) and $\alpha^a = 0.03 \text{ cm}^{-1}$ (doped with $C = 0.3 \text{ wt\%}$), and for samples from the series with Dy^{3+} at a wavelength of $1.05 \mu\text{m}$ between ion absorption bands $\alpha^a = 0.70 \text{ cm}^{-1}$ (undoped) and $\alpha^a = 0.16 \text{ cm}^{-1}$ (doped with $C = 0.3 \text{ wt\%}$). The obtained values α^a allow us to conclude that the absorption is higher in undoped samples.

Fig. 6 shows the spectral dependences of the linear refractive index of the studied glass samples near the FAB edge, calculated by the formulas (2) and (3). At the

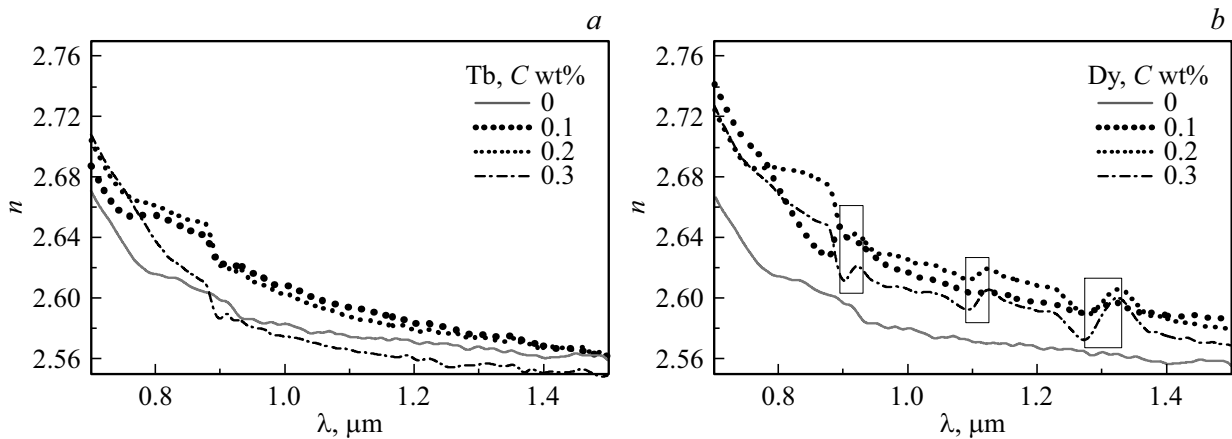


Figure 6. Spectral dependences of the linear refractive index calculated for samples of undoped glasses of the composition $\text{Ga}_5\text{Ge}_{20}\text{Sb}_{10}\text{Se}_{65}$ (solid lines) and doped with Tb^{3+} (a), and Dy^{3+} (b).

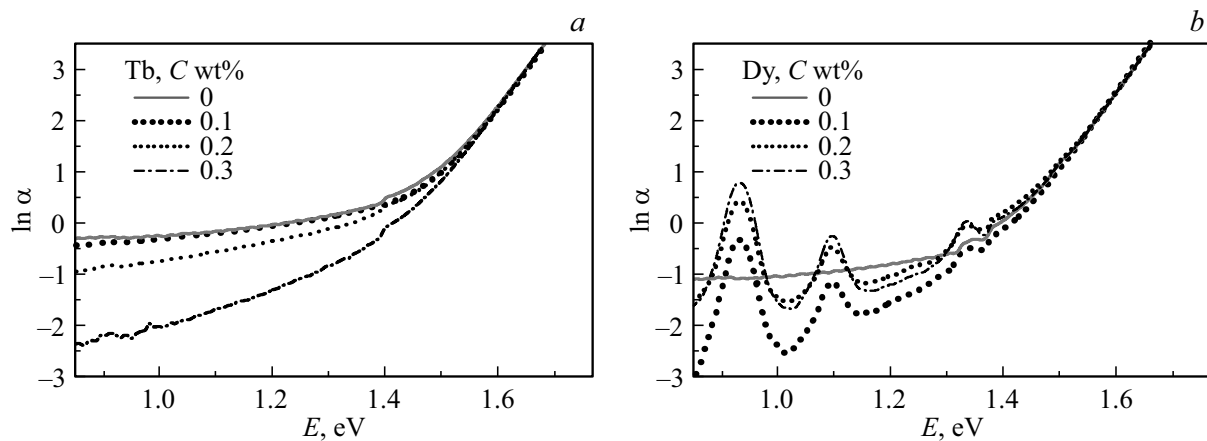


Figure 7. The logarithm of the attenuation coefficient depending on the photon energy calculated for samples of undoped chalcogenide glasses of the composition $\text{Ga}_5\text{Ge}_{20}\text{Sb}_{10}\text{Se}_{65}$ (solid lines), and doped with Tb^{3+} (a), and Dy^{3+} (b).

FAB edge, the refractive index of all samples decreases with wavelength, which corresponds to the normal dispersion of the glass, but samples with Dy^{3+} have areas of anomalous dispersion (in Fig. 5, b these areas are highlighted by rectangles), which correspond to ion absorption bands at $\lambda \approx 0.9, 1.1, 1.3 \mu\text{m}$.

The refractive index of samples with Tb^{3+} at the Urbach tail ($\lambda < 0.8 \mu\text{m}$) increases with the ion concentration, and at the weak absorption tail, there is no obvious dependence on C . For the samples with Dy^{3+} at the Urbach tail, the refractive index of the undoped sample is less than that of the doped ones, but no obvious dependence on C was revealed both at the Urbach tail and at the weak absorption tail.

Calculated by the Moss formula [23] value of the linear refractive index in the low-frequency limit ($\nu \rightarrow 0$) for the mean value of $E_g = 1.91 \text{ eV}$ (Table. 2) is $n_0 = 2.55$, which is in good agreement with the values of n presented in Fig. 6 for large λ and with the literature data [24].

3.3. Determination of parameters characterizing the FAB edge

The dependence of the function $\ln \alpha$ on the photon energy (Fig. 7) allows us to distinguish the Urbach tail and the weak absorption tail for each sample. It can be seen that for samples with Tb^{3+} , these regions are well approximated by linear functions, the slope of which can determine the parameters E_U and E_W . Samples with Dy^{3+} have ion absorption bands at the weak absorption tail. In this case, the approximating linear function is constructed from the dependence sections outside the absorption bands. The calculated values of E_U and E_W are presented in Table 2.

We note that at the Urbach tail, due to strong absorption, the scattering contribution is insignificant. Therefore, the values of E_g can be determined by the formula (7), by the absorption level $\alpha_g = 10^3 \text{ cm}^{-1}$. For the glasses doped with Dy^{3+} , the value of E'_g was determined by the level of $\alpha'_g = 70 \text{ cm}^{-1}$, and for the glasses doped with Tb^{3+} , by the level of $\alpha'_g = 50 \text{ cm}^{-1}$.

Table 2. Parameters of the edge of the FB glasses

| Activator concentration | E_g , eV ($\alpha_g = 10^3 \text{ cm}^{-1}$) | E_U , eV | E_W , eV |
|--------------------------|---|------------|------------|
| 0 wt% Tb ³⁺ | 1.92 | 0.069 | 0.72 |
| 0.1 wt% Tb ³⁺ | 1.91 | 0.066 | 0.69 |
| 0.2 wt% Tb ³⁺ | 1.91 | 0.067 | 0.48 |
| 0.3 wt% Tb ³⁺ | 1.91 | 0.066 | 0.26 |
| 0 wt% Dy ³⁺ | 1.92 | 0.067 | 0.84 |
| 0.1 wt% Dy ³⁺ | 1.90 | 0.065 | 0.20 |
| 0.2 wt% Dy ³⁺ | 1.91 | 0.067 | 0.35 |
| 0.3 wt% Dy ³⁺ | 1.90 | 0.065 | 0.33 |

According to the results presented in Table 2, the values of E_U and E_g vary within 1%, with a change in the concentration of REE ions, which is within the measurement error of the spectra. It can be concluded that these parameters practically do not change when doping glasses of this composition with an ion concentration up to 0.3 wt%. At the weak absorption tail, the attenuation coefficient is determined by the contribution of both absorption and scattering of radiation in the glass. The values of the parameter E_W differ by more than 50% for the undoped and doped glasses (Table 2, Fig. 8), and E_W is greater for the undoped samples. In samples with Tb³⁺, the value of E_W decreases with increasing ion concentration.

4. Results and discussion

As a result of the studies, it was found that doping of chalcogenide glass of the composition Ga₅Ge₂₀Sb₁₀Se₆₅ with terbium and dysprosium ions with a concentration of ≤ 0.3 wt% practically does not affect such parameters of the FAB edge of the glass as the Urbach energy and the optical band gap energy. This means that the presence of ions and crystalline inclusions in small concentrations does not affect zone-zone transitions, which determine the value of E_g . Transitions of charge carriers involving bound states near the edges of the valence band and conduction band, which determine the value of E_U , also occur independently of the crystals content and activator. This is due to a significant difference in the value of $E_g \approx 1.9$ eV obtained for this glass, and the energy of REE ion transitions at wavelengths greater than $0.8 \mu\text{m}$ (Fig. 1, c, d), not exceeding 1.55 eV. Meanwhile, according to the results obtained, such transitions occur in the region of weak absorption of glass, where the main differences in optical properties at different concentrations of the REE ion are revealed. In particular, it was found that doping of glass leads to a decrease in the parameter of the weak

absorption tail. Estimates of the contribution of scattering to the calculated values of the attenuation coefficient obtained from microstructural analysis allowed us to conclude that the absorption coefficient is greater in the undoped samples.

Since the weak absorption tail corresponds to transitions between bound states of charge carriers inside the band gap, it can be concluded that the distribution of bound states in the band gap depends on the concentration of the activator, which is a consequence of structural changes during glass doping. As noted in [14], in the glasses of the Ga–Ge–Sb–Se system, Ga and Se atoms form GaSe₄ tetrahedra, and the Ga–Se bond is closer to ionic than other heteropolar bonds, such as Ge–Se, Sb–Se, Ge–Sb. A certain number of homopolar bonds Ga–Ga should also be taken into account. During doping, trivalent REE ions are grouped near GaSe₄ tetrahedra and actually act as charge compensators. This can lead to a decrease in the density of bound states in the band gap and, accordingly, a decrease in the absorption coefficient at the weak absorption tail of the glass.

With respect to micro-dimensional crystalline inclusions, it can be assumed that, compared with the glassy state of the same composition, their electronic properties are manifested in a decrease in the probability of transitions at the Urbach tail, and the band gap energy is comparable to E_g of glass. The presence of such crystals in the glass matrix leads to the scattering of radiation, and it is found that the concentration of crystals and, accordingly, the scattering is greater in the undoped glass of the composition under consideration.

One of the possible reasons for the presence of crystals in undoped chalcogenide glasses is the presence of an oxygen impurity in the form of Ge–O, which is the germ for the growth of GeSe₂ crystals. More electropositive REE bind oxygen [13] and inhibit crystal growth.

The study of two systems of doped glasses revealed differences in the optical response near the FAB edge, depending on whether the REE ions have absorption bands

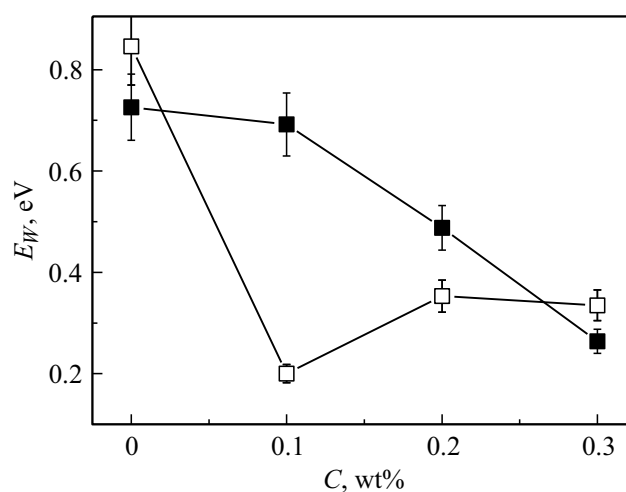


Figure 8. Parameter E_W depending on the ion concentration for samples of glasses of the composition Ga₅Ge₂₀Sb₁₀Se₆₅ doped with Tb³⁺ (■) and Dy³⁺ (□).

in this region. Thus, at the weak absorption tail of glasses with Tb^{3+} , the absorption coefficient is determined only by transitions between bound states inside the band gap of the glass, since there are no ion absorption bands here. When pumped at a wavelength of $2\ \mu m$, terbium ions practically do not interact with the glass matrix. It should be noted, that it was in optical fibers made of glasses with Tb^{3+} that the generation of laser radiation in the mid IR range (at wavelengths 5.25 and $5.38\ \mu m$) was first obtained [5,6]. Glasses with Dy^{3+} have absorption bands at the weak absorption tail of the glass. Therefore, when pumping at wavelengths less than $2\ \mu m$, energy transfer between ions and bound states in the band gap is possible. It can be assumed that it is for this reason that terbium ions in selenide glasses have a luminescence lifetime in the mid IR range several times higher than that of dysprosium ions [4].

5. Conclusion

It has been found, that doping of chalcogenide glasses of the composition $Ga_5Ge_{20}Sb_{10}Se_{65}$ with terbium and dysprosium ions in low concentrations (up to 0.3 wt%) practically does not affect the optical properties of the glasses at the Urbach tail and the bandgap energy, but at the weak absorption tail, the optical response of the glasses depends on the concentration of the activator. In particular, in this region, at a given wavelength, the absorption coefficient is greater for undoped glass (outside the absorption band of the REE ion).

It is shown that in glasses with dysprosium in the region of weak absorption, the optical response is formed not only by the glass matrix, but also by transitions between the energy levels of dysprosium ions. The possible transfer of energy between ions and bound states in the band gap of glass can lead to the extinction of luminescence, which must be taken into account when developing laser devices based on such glasses.

Funding

The results were obtained during the implementation of the project 21-13-00194 of the Russian Science Foundation.

Conflict of interest

The authors declare that they have no conflict of interest.

References

- [1] V.S. Minaev. *Stekloobraznye poluprovodnikovye splavy* (Metallurgiya, Moscow, 1991). (in Russian).
- [2] H. Guo, J. Cui, C. Xu, Yantao Xu, G. Farrell. In: *Mid-Infrared Fluoride and Chalcogenide Glasses and Fibers. Progress in Optical Science and Photonics*. V. 18 (Springer, Singapore, 2022). DOI: 10.1007/978-981-16-7941-4_7
- [3] S.D. Jackson, R.K. Jain. *Opt. Express*, **28** (21), 30964–31019 (2020). DOI: 0.1364/OE.400003
- [4] M.F. Churbanov, B.I. Denker, B.I. Galagan, V.V. Koltashev, V.G. Plotnichenko, M.V. Sukhanov, S.E. Sverchkov, A.P. Velmuzhov. *J. Lumin.*, **245**, 118756 (2022). DOI: 10.1016/j.jlumin.2022.118756
- [5] V.S. Shiryaev, M.V. Sukhanov, A.P. Velmuzhov, E.V. Karaksina, T.V. Kotereva, G.E. Snopatin, B.I. Denker, B.I. Galagan, S.E. Sverchkov, V.V. Koltashev, V.G. Plotnichenko. *J. Non-Cryst. Solids*, **567**, 120939 (2021). DOI: 10.1016/j.jnoncrysol.2021.120939
- [6] B.I. Denker, B.I. Galagan, V.V. Koltashev, V.G. Plotnichenko, G.E. Snopatin, M.V. Sukhanov, S.E. Sverchkov, A.P. Velmuzhov. *Opt. Laser Technol.*, **154**, 108355 (2022). DOI: 10.1016/j.optlastec.2022.108355
- [7] A.P. Velmuzhov, M.V. Sukhanov, T.V. Kotereva, N.S. Zernova, V.S. Shiryaev, E.V. Karaksina, B.S. Stepanov, M.F. Churbanov. *J. Non-Cryst. Solids*, **517**, 70–75 (2019). DOI: 10.1016/j.jnoncrysol.2019.04.043
- [8] Virginie Nazabal, Jean-Luc Adam. *Opt. Mater.: X*, **15**, 100168 (2022). DOI: 10.1016/j.omx.2022.100168
- [9] A. Zakery, S.R. Elliot. *Optical nonlinearities in chalcogenide glasses and their applications* (Springer, Berlin, 2007).
- [10] S.G. Bishop, D.A. Turnbull, B.G. Aitken. *J. Non-Crystal. Solids*, **266–269**, 876–883 (2000). DOI: 10.1016/S0022-3093(99)00859-5
- [11] *MID-INFRARED FIBER PHOTONICS: Glass Materials, Fiber Fabrication and Processing, Laser and Nonlinear Sources*. Ed. by: S. Jackson, R. Vallee, M. Bernier (Woodhead Publishing, 2021).
- [12] V.S. Shiryaev, A.I. Filatov, E.V. Karaksina, A.V. Nezhdanov. *J. Sol. St. Chem.*, **303**, 122454 (2021). DOI: 10.1016/j.jssc.2021.122454
- [13] M.V. Sukhanov, A.P. Velmuzhov, P.A. Otopkova, L.A. Ketkova, I.I. Evdokimov, A.E. Kurganova, V.G. Plotnichenko, V.S. Shiryaev. *J. Non-Cryst. Solids*, **593**, 121793 (2022). DOI: 10.1016/j.jnoncrysol.2022.121793
- [14] I.I. Evdokimov, D.A. Fadeeva, A.E. Kurganova, V.S. Shiryaev, V.G. Pimenov, E.V. Karaksina. *J. Analyt. Chem.*, **7** (7), 869–877 (2020). DOI: 10.1134/S1061934820070060
- [15] Yu.S. Kuzuyutkina, E.A. Romanova, V.I. Kochubey, V.S. Shiryaev. *Opt. i spektr.*, **117** (1), 60–66 (2014). (in Russian).
- [16] L. Sojka, Z. Tang, H. Zhu, E. Beres-Pawlik, D. Furniss, A.B. Seddon, T.M. Benson, S. Sujecki. *Opt. Mater. Express*, **2** (11), 1632–1640 (2012). DOI: 10.1364/OME.2.001632
- [17] M.F. Churbanov, B.I. Denker, B.I. Galagan, V.V. Koltashev, V.G. Plotnichenko, M.V. Sukhanov, S.E. Sverchkov, A.P. Velmuzhov. *J. Luminesc.*, **231**, 117809 (2021). DOI: 10.1016/j.jlumin.2020.117809
- [18] J. Ren, G. Yang, H. Zeng, X. Zhang, Y. Yang, G. Chen. *J. Am. Ceram. Soc.*, **89**, 2486–2491 (2006). DOI:10.1111/j.1551-2916.2006.01070.x
- [19] F. Starecki, G. Louvet, J. Ari, A. Braud, J.-L. Doualan, R. Chahal, I. Hafienne, C. Boussard-Pledel, V. Nazabal, P. Camy. *J. Luminesc.*, **218**, 116853 (2020). DOI: 10.1016/j.jlumin.2019.116853
- [20] F. Starecki, F. Charpentier, J.-L. Doualan, L. Quetel, K. Michel, R. Chahal, J. Troles, B. Bureau, A. Braud, P. Camy, V. Moizan, V. Nazabal. *Sens. Actuators B*, **207**, 518 (2015). DOI: 10.1016/j.snb.2014.10.011
- [21] L.A. Ketkova, A.P. Velmuzhov, M.V. Sukhanov, B.S. Stepanov. *J. Eur. Ceramic Soc.*, **41**, 7852–7861 (2021). DOI: 10.1016/j.jeurceramsoc.2021.08.019

- [22] J. Tauc. *Amorphous and Liquid Semiconductors* (Plenum, London, 1974).
- [23] T. Moss, G. Burrell, B. Ellis. *Semiconductor optoelectronics* (1976).
- [24] F. Starecki, N. Abdellaoui, A. Braud, J.-L. Doualan, C. Boussard-Plédel, B. Bureau, P. Camy, V. Nazabal. *Opt. Lett.*, **43** (6), 1211–1214 (2018).
DOI: 10.1364/OL.43.001211